Title
THE TOTAL CROSS SECTIONS FOR 190-Mev POSITIVELY CHARGED K MESONS IN COMPLEX NUCLEI

Author
Kerth, Leroy Thomas.

Publication Date
1957-04-08

UCRL-3747

UNIVERSITY OF
CALIFORNIA

Radiation
Laboratory

THE TOTAL CROSS SECTIONS FOR 190-Mev POSITIVELY CHARGED K MESONS IN COMPLEX NUCLEI

BERKELEY, CALIFORNIA

DISCLAIMER

UCRL-3747
Physics

UNIVERSITY OF CALIFORNIA

Radiation Laboratory
Berkeley, California

Contract No. W-7405-eng-48

THE TOTAL CROSS SECTIONS FOR 190-Mev POSITIVELY CHARGED K MESONS IN COMPLEX NUCLEI

(Thesis)

Leroy Thomas Kerth

April 8, 1957

Printed for the U.S. Atomic Energy Commission

Contents

Abstract 3
I. Introduction 4
II. Measurement of the Cross Section
A. Physical Arrangement and Experimental Procedure . . 5
1. K^+-meson beams 5
2. Description of the counters 7
3. Electronics and data recording 10
4. Counter functions 11
5. Procedure 13
B. Reduction of Data
1. Film reading 15
2. Calculation of the cross sections 16
C. Corrections
1. Decay in flight 17
2. Multiple scattering 18
III. The Cross Sections 21
IV. Complex Square-Well Analysis
A. Formulation of the Problem 24
B. Optical Model (W.K.B. Method) 25
C. Effect of Coulomb Potential 29
D. Inelastic Scattering Correction 30
E. Complex Square-Well Parameters 31
F. Mean Free Path for Interaction in Nuclear Matter . . . 33
V. Discussion
A. Real Potential 36
B. Absorption 36
1. Surface effect 36
2. Effect of magic numbers 36
3. Conclusion 36
Acknowledgments 37
Appendix 38

THE TOTAL CROSS SECTIONS FOR 190-Mev POSITIVELY CHARGED K MESONS IN COMPLEX NUCLEI

Leroy Thomas Kerth

Radiation Laboratory
University of California
Berkeley, California

April 8, 1957

ABSTRACT

The attenuation cross section and the differential scattering cross section in one angular interval were measured for K^+ mesons of 192 Mev kinetic energy. The targets were carbon, aluminum, copper, silver, and lead.

The cross sections were analyzed in terms of the optical model to determine the real and imaginary potentials. The average real potential was found to be 24 Mev. The mean free path in nuclear matter was found to be consistent with a K^+-nucleon scattering cross section of about 10 millibarns. Some evidence was found for a variation of the mean free path in nuclear matter with Z.

I. INTRODUCTION

One of the basic problems of physics is concerned with the forces that exist in nature. With the discovery of a new particle, one of the first questions that arises is, how does it interact with other particles? The early experiments, carried out with the Bevatron, gave valuable information concerning the basic properties of K mesons such as decay modes, mean life, and Mass.[1] Such experiments showed an almost complete degeneracy among the K mesons of different decay modes. Experiments with nuclear emulsions have shown that to a rather good approximation the K's with different decay modes interact with nuclear matter in the same way.[2] Thus, it was felt that an experiment to measure the total elastic and inelastic scattering cross sections of positive K mesons, in several pure materials, would be of interest in learning the role of K mesons in nature.

II. MEASUREMENTS OF THE CROSS SECTIONS

The nuclei chosen for the measurement were carbon, aluminum, copper, silver, and lead. The thickness of the targets was chosen so as to have equal energy loss by the K mesons in each target. The K mesons produced in the Bevatron were momentum-analyzed and focused on the scattering target. The K particles were selected from the background in the momentum-analyzed beam by velocity-sensitive counters. A scattering event was determined by counters placed after the target to indicate the absorption or scatter of a K particle.

A. Physical Arrangement and Experimental Procedure

1. K^+ beams

The arrangement of the K^+ beam is shown in Fig. 1. The K^+ mesons were produced by the 6.2-Bev proton beam striking either a carbon or a polyethylene target. (These targets were used so as to be compatible with antiproton experiments running concurrently on the Bevatron). The K mesons of momentum 500 Mev/c produced at 0^o were bent through approximately 45^o in the magnetic field of the Bevatron, and then left the vacuum through a 0.020-inch-thick dural window. A three-element quadrupole strong-focusing lens[3] was placed as close as possible to the window. An analyzing magnet, immediately after the quadrupole, was used to select the desired momentum.

The momentum analysis and focusing properties of the Bevatron field produce for each momentum a virtual image as shown in Fig. 1. The quadrupole lens and analyzing magnet together form a "Strong-Focusing Spectrometer."[1,4] This spectrometer is adjusted to use the virtual images produced by the Bevatron field as objects, and produce a set of real images at the counter array.

The momentum resolution and the momentum spread can be adjusted over wide limits by varying the magnetic fields of the strong-focusing spectrometer. The subject of particle focusing is a vast one and shall not be covered here.

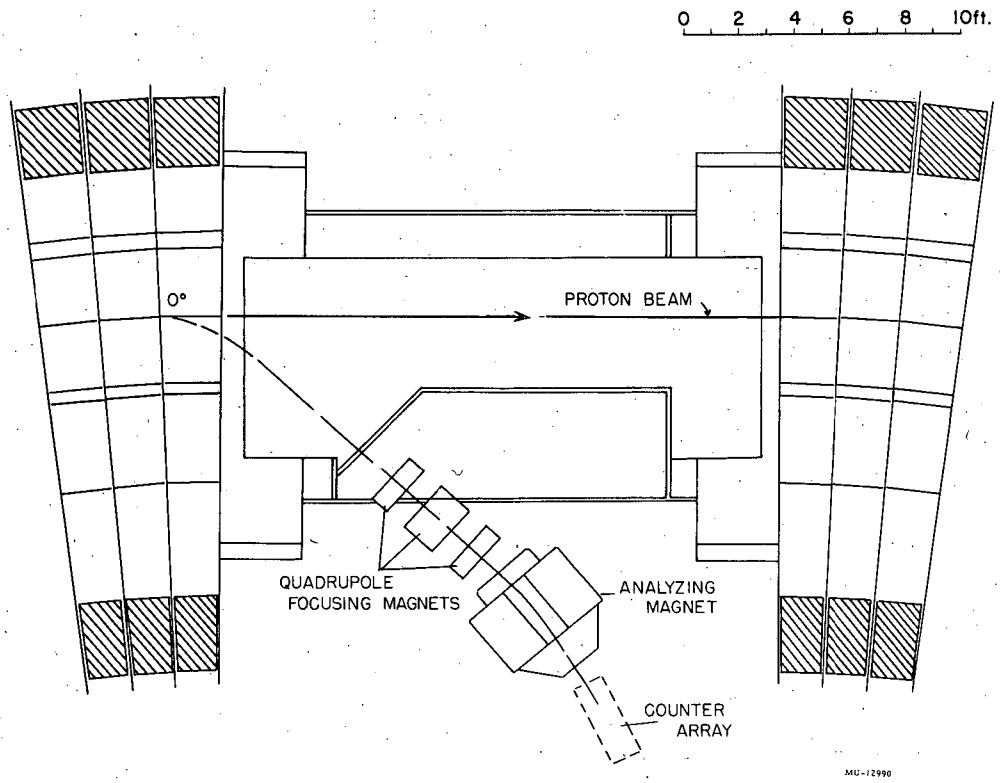

Fig. 1. The K^+ beam. The heavy concrete shielding that surrounded the entire apparatus is not shown.

The experimental arrangement gave a beam of 192 Mev kinetic energy at the scattering target with a spread of ± 25 Mev. The flux was about 10 K particles per square inch per 10^{10} protons on the production target, with an angular divergence of $\pm 3^{\circ}$.

2. Description of the Counters

The function of the counter arrangement was threefold: (a) To define the direction of the K particles, (b) to select from the momentum-analyzed beam those particles with the proper velocity to have the mass of a K meson, (c) to determine the fraction of these particles that scattered or interacted in the target.

Figure 2 shows a schematic layout of the counters. For the sake of clarity, only the sensitive region of the counters has been shown. Angular definition of the particles was provided by two scintillation counters D_1 and D_2, 1.25 inch in diameter and 0.25 inch thick in the beam direction. These were placed approximately 2 feet apart to define the direction of the incident particles to a cone of 3° half angle.

Two Cerenkov counters were used to define the velocity of the particles. The K mesons in the beam are accompanied by a background of protons and pions of the same momentum. The use of velocity and $H\rho$ to select particles of a given mass is quite common.[5] The first counter in the array is a Cerenkov counter using as a radiator Fluorochemical 0-75 manufactured by Minnesota Mining and Manufacturing Company. It is a clear liquid with an index of refraction of 1.275. The photomultiplier is placed so as to detect the light emitted at all angles. Thus, the counter is sensitive to all particles with $\beta \geq 0.8$.

The second Cerenkov counter, placed directly behind the first defining counter, used a radiator of carbon disulphide. The index of refraction of CS_2 is 1.62, so that particles with $\beta \geq 0.617$ produce radiation. In addition, this counter has an upper limit on β because an air space is left between the radiator and the photomultiplier (Fig. 3). Thus, light emitted at an angle greater than arcsin (1/n) is internally reflected and does not strike the photomultiplier tube. The upper limit of the counter is given by

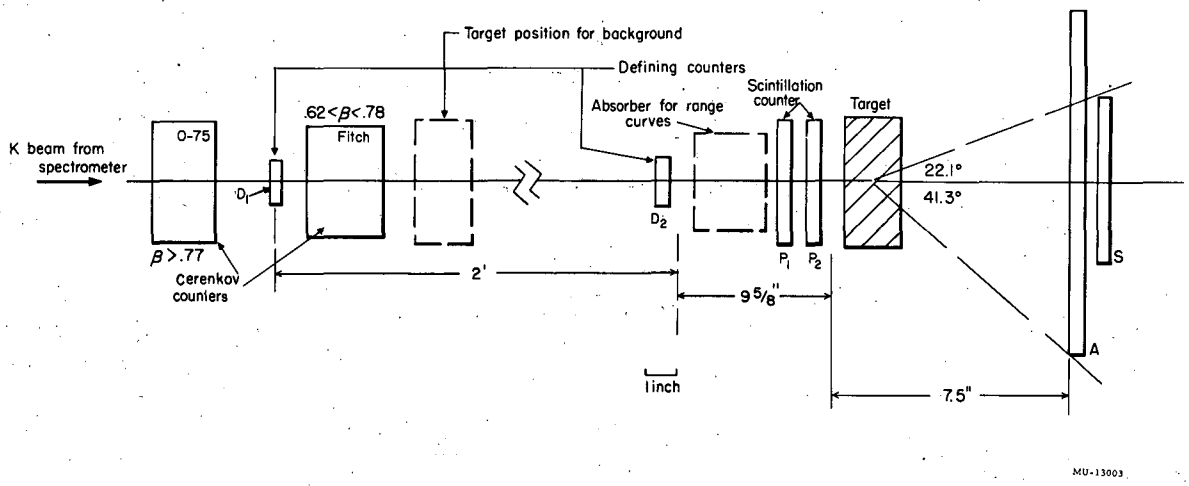

Fig. 2. Counter arrangement.

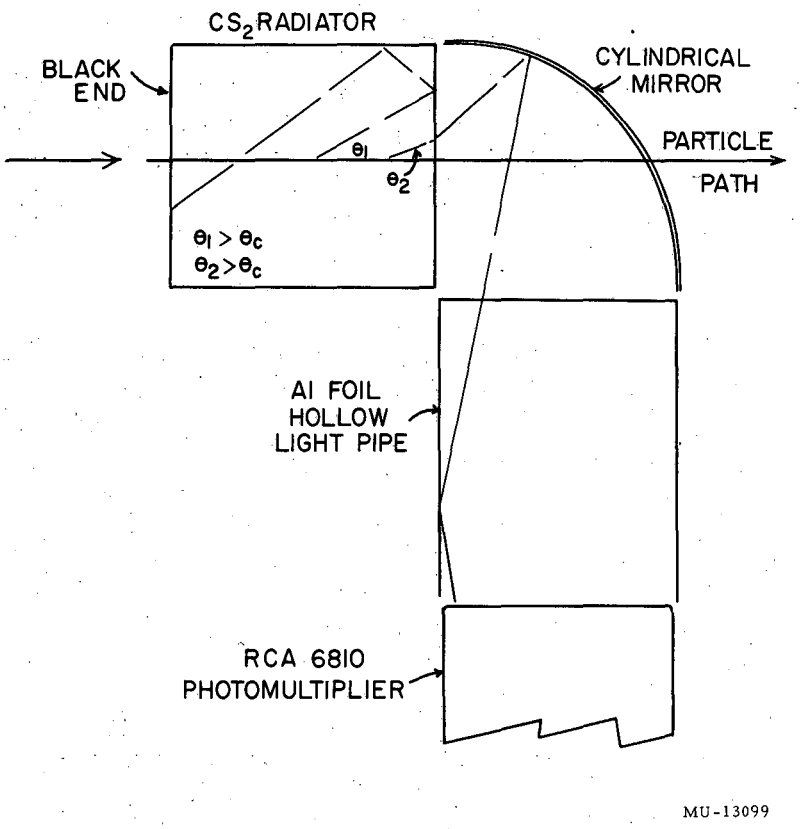

Fig. 3. Schematic drawing of the Fitch counter.

$$\beta = \frac{1}{n \cos \theta_c} ,$$

where θ_c = arcsin (1/n), n = index of refraction. This counter was first described by Fitch,[6] and is commonly called a Fitch counter.

The height of the pulses from the two defining counters was recorded as a further measure of the velocity.

The scintillation counters P_1 and P_2 (Fig. 2) were used in conjunction with the absorber in taking range curves to determine the energy of the incident beam and to test for contamination of the incident K beam.

The scattering targets were placed either just behind the P_2 counter or behind the velocity-interval Cerenkov counter (Fitch counter). The latter position was used for a background measurement (which is described more fully in Section I-A-5).

The counters, S and A, were scintillation counters 6.75 and 11.5 inches in diameter respectively. The half angles subtended by these counters at the target were 22.1^{o} and 41.3^{o}.

3. Electronics and Data Recording

Each of the counters used one RCA 6810 photomultiplier tube, with the exception of the two P counters, which each used one RCA 1P21 photomultiplier, and the S counter, which used four RCA 1P21's. The Fitch counter and the two defining counters were wired so that a positive signal was available from the last dynode as well as a negative one from the anode. The anode signals from the 0-75, Fitch, defining, P_1, and P_2 counters were amplified with Hewlett-Packard 460A distributive amplifiers and connected to a six-channel coincidence circuit.[7] This circuit is similar to that described by Garwin.[8] It allows one to mix any combination of the six inputs into two separate circuits. Also, an anticoincidence between the outputs of the two circuits is made without destroying either of the two coincidence signals. Since particularly short resolution times were not needed, no attempt was made to push the circuit to its maximum resolution. Delay curves taken during the run indicated a resolution time of about 2×10^{-8} sec.

The outputs of the coincidence circuits were monitored with Hewlett-Packard prescalers (about 10^{-7} second resolution time for CW) followed by conventional 1-microsecond scalers. The anticoincidence circuit was monitored directly with a 1-microsecond scaler.

The output from the anticoincidence was used to trigger the sweep of a Tektronix 517 Oscilloscope. The dynode pulses from the Fitch and defining counters, along with the pulses from the S and A counters, were mixed after suitable delays and displayed on the sweep of the oscilloscope. The sweeps were recorded photographically by means of a Du Mont 35-mm moving-film camera. It was necessary to record 10 to 20 sweeps during the 100 milliseconds of beam pulse. Thus, the camera was pulsed so as to move the film about 6 inches during each pulse and remained stationary between pulses.

The photographic record allowed pulse-height and timing measurements to be made on each sweep.

4. Counter Functions

The composition of the momentum-analyzed beam was approximately 400 pions and 200 protons to one K meson. The K^+ cross sections are a small fraction of the pion or proton cross sections. Therefore, it was necessary for the counters to identify K particles with a contamination of pions and protons of less than 1%.

In the momentum-selected beam the pions have a β of >0.78, so that they should count in the 0-75 but not the Fitch counter. The K particles have a β of 0.71, so that they should count in the Fitch counter only. The protons should count in neither.

The contamination of pions was measured for various combinations of the counters by varying the thickness of the copper absorber in front of the P_1 and P_2 counters and observing the coincidence rate between counters P_1 and P_2 and the identified K mesons. Since for pions and K particles of the same momentum the range of the pions is much greater, we expect the coincidence rate to drop sharply with an absorber thickness greater than the range of the K mesons. One set of such data is presented in Fig. 4. From such data, it was determined that the contamination

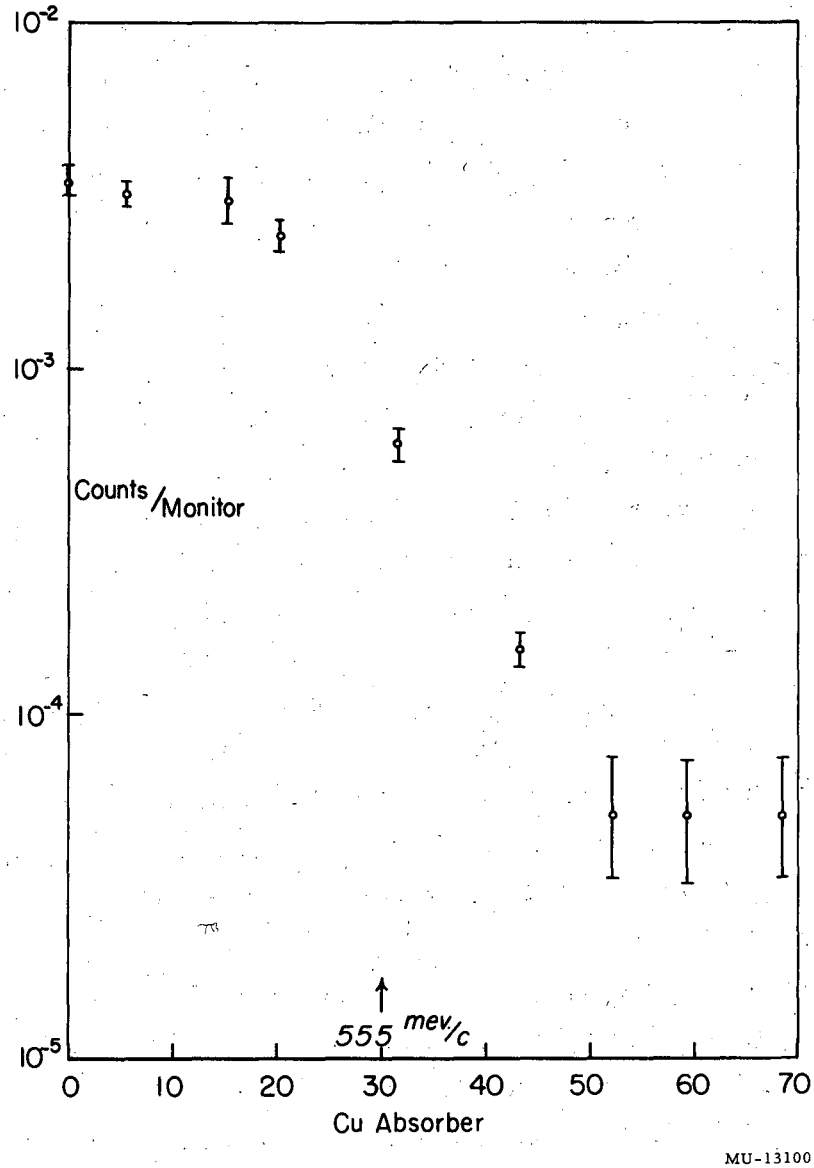

Fig. 4. Counting rate vs range.

due to pions was less than 1% of the K flux when the Fitch counter was used in coincidence with the defining counters and the 0-75 counter was in anticoincidence. It was estimated that the 0-75 counter missed less than one in 10^4 of the pions.

In spite of the absolute lower limit of the Fitch counter, a small contamination of protons was discovered. The proton contamination resulted from a true coincidence of the proton between the defining counters and an accidental coincidence with a pion giving a count in the Fitch counter. This contamination was determined from the pulse-height spectra of the two defining counters. A typical set of pulse-height data is given in Fig. 5. A point is placed on the graph for each combination of pulses. The density of dots indicates the pulse-height peaks. The group of pulses at low pulse heights was attributed to K particles, while the other group was assumed to be protons.

By accepting only particles that excited the Fitch counter, did not excite the 0-75 counter, and gave pulse heights in the two defining counters within the limits set in Fig. 5, we selected K particles with less than 1% contamination of other particles.

5. Procedure

One of the targets was placed in position either directly behind the P_2 counter, or after the Fitch counter. Several thousand traces were recorded and then another target was used.

The main source of background was due to K particles that decayed in flight between the P_2 counter and the S counter. Using a mean life for the K particle of 1.3×10^{-8} second,[9] we find that about 6% of the K particles decay. Since the fraction of particles that interact is about 3%, the background measurement should be as exact as possible so as not to introduce large systematic errors.

The fraction of K particles that decay while traversing a given distance is $F = \exp - \ell/L$, where L is the mean flight distance given by $L = \beta\gamma c\tau$. The quantities β, γ, and c have their usual meanings; τ is the mean life of the particles. We see that the decay fraction is a function of $\beta\gamma$ or the momentum of the K. So as to have F the same

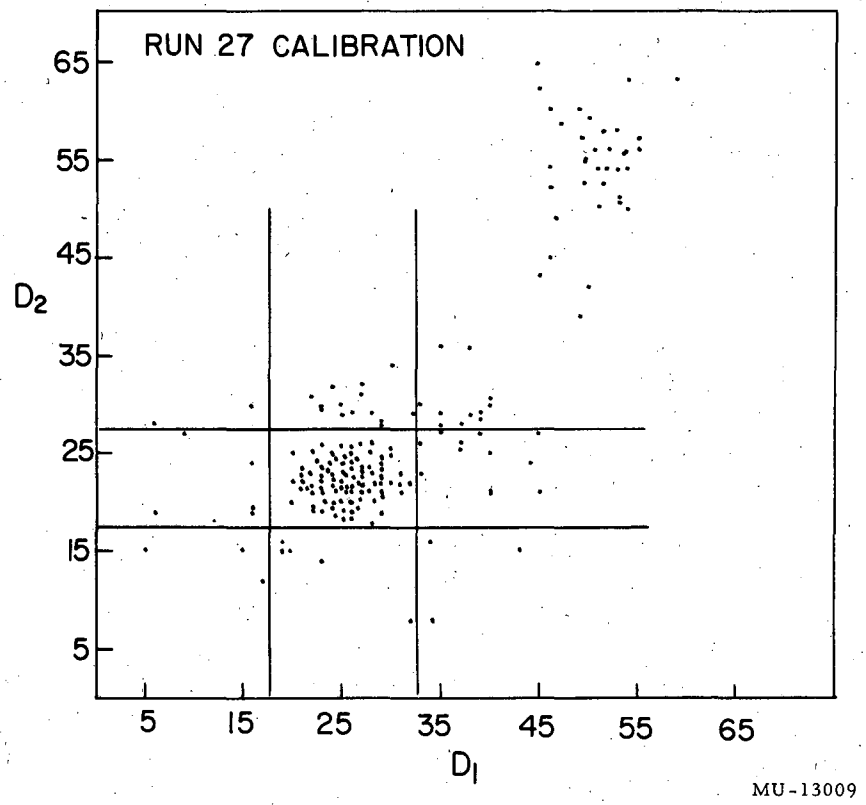

Fig. 5. Pulse-height distribution for the defining counters.

for the background measurement and the measurement of the effect, it was necessary for the particles to have the same momentum at corresponding points between the P_2 and S counters.

For the target thicknesses that were chosen, the K particles lost about 30 Mev in traversing the target. Simply removing the target would have given a different condition for the background measurement than for the effect with the target in place. To circumvent this unfortunate state of affairs, it was decided to make the background measurement by placing one of the targets (they all have the same stopping power) in the position immediately behind the Fitch counter. Such a procedure is only a first approximation to the desired condition, and further corrections are discussed in Section III-C-1.

B. Reduction of the Data

1. Film Reading

Calibration of the pulse height from the two defining counters was accomplished by measuring the heights of the pulses in arbitrary units, using a standard microfilm reader. The calibration was carried out at various times, to check for any drift in gain of the photomiltipliers or amplifiers. It was found that the system was quite stable.

After the limits on pulse height had been determined, charts were made up showing the limits and the positions in time of each pulse on the sweep. The timing of a pulse could be read with an accuracy of approximately 5×10^{-9} sec. Thus the time criteria imposed during the film reading improved the coincidence-resolving time. Each sweep, as viewed with the microfilm viewer, was compared with the chart, and the scanner quickly determined whether or not the event was caused by a K particle. If it was a K, the sweep was examined for pulses from the S and A counters. The sweeps were then classified as one of the following:

(1) out; (2) K; (3) K, A; (4) K, S; (5) F.

These were defined as follows:

out - Events that did not fit the pulse height or time criteria

K - Events that fitted pulse-height criteria but that had neither an S or A count

K,A - Events that fitted the criteria for a K and triggered the A counter

K,S - Events that fitted the criteria and triggered both the S and A counters

F - Events that fitted the criteria and triggered only the S counter

The last four of these are of interest. A K sweep results from an event giving no charged particle within 41° of the beam. A K, A event results from a scatter into the angular interval between 22.1° and 41.3°. The KS events result from particles that scatter less than 21.1° with respect to the beam. The F gives a measure of the accidental rate of the large counters because an oops can occur only by an accidental coincidence between a K scatter and a random count from the S counter.

The procedure was to read through the film, counting the number of events in each of the classes. When a length of film was scanned, the above numbers were recorded along with the film number. The scanners were not allowed to know which film went with which target. Each set of such data was reduced to a cross section as described in the next section. These cross sections were then compared, and the deviation between them was found to be compatible with the statistics of each. Thus, it was felt that the scanners were not introducing subjective errors.

2. Calculation of the Cross Sections

From the various numbers recorded during the film reading, three cross sections can be calculated. First, σ_1 for 21° geometry; second, σ_2 for 41° geometry, and thirdly, $\Delta\sigma$, the differential cross section between 21° and 41°. These cross sections are given by

$$\sigma_1 = \frac{1}{\eta}\left(\ln\frac{N_0}{N_1} - \ln\frac{N_0'}{N_1}\right),$$

$$\sigma_2 = \frac{1}{\eta}\left(\ln\frac{N_0}{N_2} - \ln\frac{N_0'}{N_2'}\right), \qquad (1)$$

$$\Delta\sigma = \frac{1}{\eta}\left(\ln\frac{N_1}{N_2} - \ln\frac{N_1'}{N_2'}\right),$$

where

$N_0 = \overline{K} + \overline{K,A} + \overline{K,S}$,

$N_1 = \overline{K,S}$,

$N_2 = \overline{K,S} + \overline{K,A}$,

$\overline{K}$ = number of K events in a given run,

$\overline{K,S}$ = number of K,S events in a given run,

$\overline{K,A}$ = number of K,A events in a given run,

primes denote background data,

η = thickness of the target in atoms/cm^2 .

The statistical standard deviation on each of the cross sections is given by the formula

$$\text{standard deviation on } \sigma_i = \sqrt{\frac{1}{N_0} - \frac{1}{N_i} + \frac{1}{N_0'} + \frac{1}{N_2'}} .$$

(For the derivation of this formula see Appendix A.)

C. Corrections

1. Decay in Flight

The technique of measuring the background described earlier accounts exactly for the decay in flight of particles that decay between the back of the target and the S or A counters. For particles that decay between the P_2 counter and the back of the target, the two arrangements are not quite the same, since the particles lose energy in the region between P_2 and the back of the target in the one case and not in the other.

Thus, the fraction of K particles that decay is greater for the background case than for the target. A correction was calculated and applied to the data. It accounted for an increase of σ_1 of 1.6% and for an increase of σ_2 of 1.9%.

A further correction must be applied to account for π- and μ-meson contamination arising from K_{π_2} and K_{μ_2} particles that decay between the last defining counter and the target, and trigger P_1 and P_2. The fraction of such decays that strikes the back counters depends again on the momentum.

The secondary particles that do strike the A and S counters have passed through the target and interacted according to a cross section different than that for K particles. These corrections amount to an increase in σ_1 and σ_2 cross sections of 1.8% and 5.5% respectively.

The total corrections arising from decay in flight then become 3.4% for σ_1 and 7.4% for σ_2.

2. Multiple Scattering

In principle, in an attenuation experiment, one would like to define the incident beam very well, then measure the total cross sections under "good geometry" (small angle subtended by the back counters). Firstly, the angular resolution of the incident beam must be compatible with sufficient flux for reasonable statistical accuracy, and secondly, a good geometry measures the multiple Coulomb scattering. The multiple scattering at small angles is large; if included in the measurement of the cross section, it would completely mask the nuclear scattering. The root-mean-square scattering angle is given by

$$\sqrt{\overline{\phi^2}} = \sqrt{b Z \Delta E} / P , \qquad (2)$$

where

Z is the charge of the scattering nucleus,

ΔE is the energy loss in traversing the target,

P is the mean momentum in the target,

b is a slowly varying function of the $\beta\gamma$ of the particle (and is given in Fig. 6).

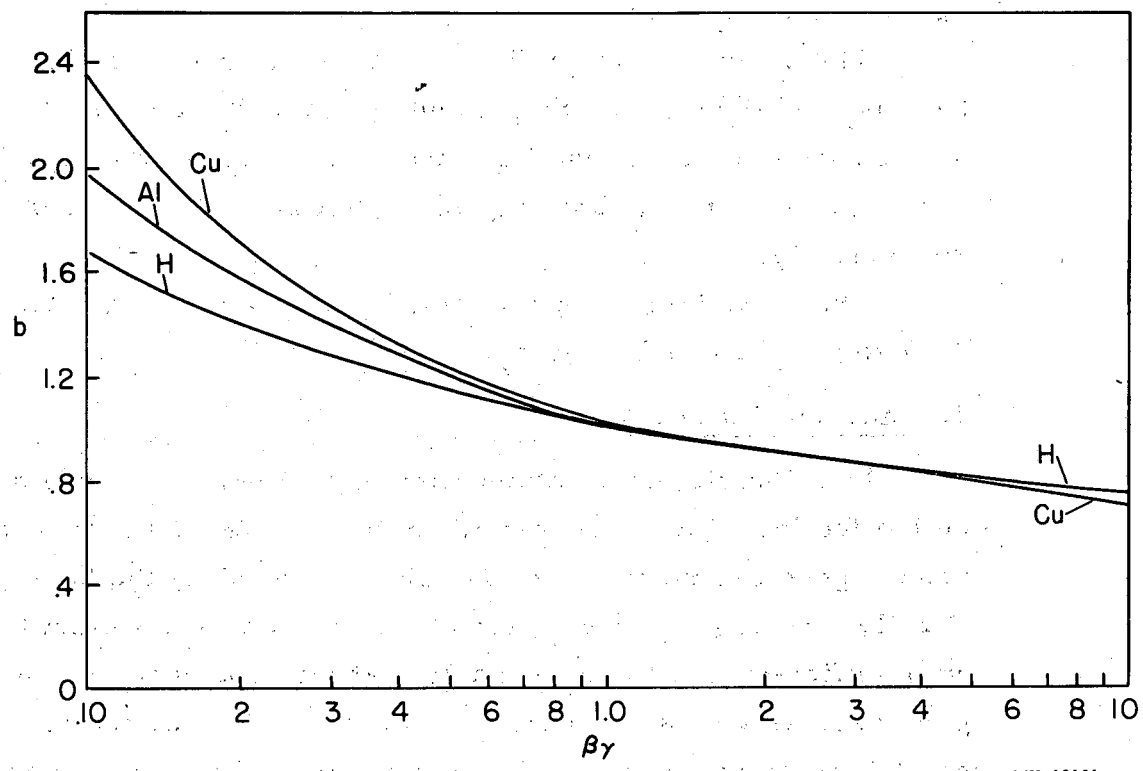

Fig. 6. b vs. $\beta\gamma$; $b = \dfrac{\overline{\phi^2}\, P^2}{Z\,\Delta E}$.

Equation (2) is easily derived by dividing the usual expression for $\sqrt{\overline{\phi^2}}^{10}$ by the dE/dx^{10}, and assuming small energy losses to that we have $\Delta E = (dE/dx)\, t$, where t is the thickness of the scatter.

Equation (2) gives, for lead, $\sqrt{\overline{\phi^2}} = 5^o$. The lower-Z targets give smaller values. The angle subtended by the S counter was about three times the standard deviation of the multiple-scattering distribution when the divergence of the incident beam was included. The calculated correction due to multiple scattering was about 0.2%.

III. THE CROSS SECTIONS

The measured cross sections are given in Table I. The uncorrected data are given in Appendix B. Columns 2 through 4 give the measured cross sections. In the analysis which follows, the useful numbers are σ/σ_g, where $\sigma_g = \pi R^2$ and R is the radius of the nucleus. R was assumed to be given by $r_0 A^{1/3}$, with $r_0 = 1.41 \times 10^{-13}$ cm. In the analysis, the initial state is assumed to be represented by a plane wave, and does not allow for the distortion of the wave by the Coulomb potential. A classical correction, to allow for the suppression of the wave at the nucleus, can be calculated on the basis of the classical orbits.[11] In Fig. 7, we see that the trajectories that just strike the edge of a nucleus of radius R are actually contained in a cross section of area πb^2. Using the classical expressions for the orbits, we find $b^2 = R^2/(1 + Vc/T)$, where $V_c = (Ze^2)/R$ is the Coulomb potential at the radius R, and T is the kinetic energy of the incident particle. The values of πb^2 are given in Table I, as well as the cross sections divided by πb^2.

Table I

The Measured Cross Sections for K Mesons in the Several Nucli (in Millibarns)

Target	C	Al	Cu	Ag	Pb
σ_1	96.5 ± 8.5	208 ± 13	505 ± 28	578 ± 38	1081 ± 86
σ_2	83 ± 6	148 ± 11	384 ± 20	451 ± 29	749 ± 62
$\Delta\sigma$	13.0 ± 3.0	51 ± 5	123 ± 12	125 ± 15	340 ± 45
πb^2	324	543	939	1320	2190
$\frac{\sigma_1}{\pi b^2}$	0.298 ± 0.026	0.383 ± 0.024	0.538 ± 0.030	0.438 ± 0.029	0.495 ± 0.039
$\frac{\sigma_2}{\pi b^2}$	0.256 ± 0.019	0.272 ± 0.020	0.408 ± 0.021	0.342 ± 0.022	0.342 ± 0.028
$\frac{\Delta\sigma}{\pi b^2}$	0.040 ± 0.009	0.094 ± 0.009	0.132 ± 0.013	0.095 ± 0.012	0.155 ± 0.021

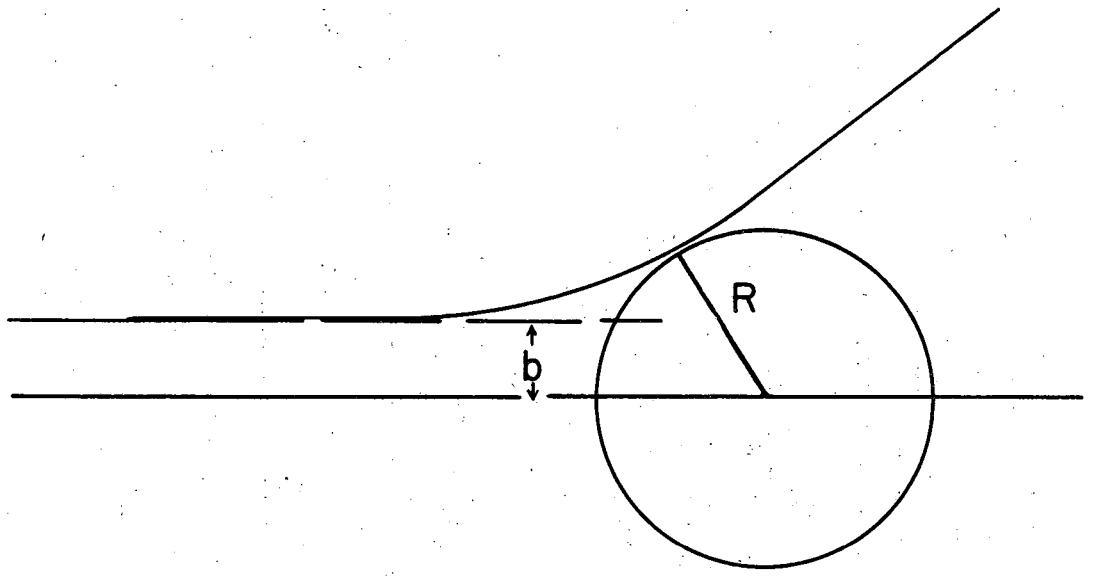

MU-13102

Fig. 7. Classical Coulomb orbits for estimating the distortion of the incident plane wave.

IV. COMPLEX SQUARE-WELL ANALYSIS

A. Formulation of the Problem

The measured cross sections are actually combinations of two different effects. Thus, we can write

$$\sigma_1 = \alpha_1 \sigma_s + \beta_1 \sigma_I ,$$

$$\sigma_2 = \alpha_2 \sigma_s + \beta_2 \sigma_I , \qquad (3)$$

$$\Delta\sigma = \Delta\alpha\sigma_s + \Delta\beta\sigma_I ,$$

where σ_s is the total coherent or elastic scattering cross section and σ_I is the total incoherent scattering, which includes all processes--such as charge exchange and inelastic scattering--that remove particles from the incident plane wave. The α's and β's are the fractions of the total elastic and total inelastic scattering cross sections included in the measurement. We now assume that the force between the K meson and the nucleus may be represented by a potential function given by

$$\begin{aligned} V &= V_1 + iV_2, \quad r < R \\ V &= 0 \qquad\qquad r > R \end{aligned} \qquad (4)$$

where V_1 and V_2 are real and independent of r. The potential of Eq. (4) is called the complex square-well potential. Evidence from experiments with nuclear emulsion have indicated that the real part of the potential is positive.[12] Thus, no attempt was made to fit the data with a negative potential.

We now assume that the initial state is given by a plane wave. Using the Schroedinger wave equation, one can calculate the exact phase shifts;[13] however, such calculations are quite laborious and are beyond the scope of this paper.

B. Optical Model

The optical model by Fernbach, Serber, and Taylor gives approximate solutions valid for small reflection and refraction at the boundary of the potential.[14]

The wave number inside the potential well is given by

$$k' = k + k_1 = k(1 + V_1/E)^{1/2}, \tag{6}$$

where k is the wave number outside the well ($k = P/\pi$) and V_1 is the real part of the potential given in Eq. (4). If we consider the optical analogy to the above problem,[15] k_1 is analogous to the real part of the index of refraction. We may also introduce the imaginary part of the index of refraction, which is the absorption coefficient K.

In complete analogy to the optical problem, Fernbach, Serber, and Taylor[14] obtain, for σ_I and σ_s,

$$\sigma_I = 2\pi \int_0^R (1 - \exp 2KS)\, \rho d\rho \tag{7}$$

or

$$\frac{\sigma_I}{\pi R^2} = \left\{1 - \left[1 - (1 + 2x) \exp 2x\right] / 2x^2\right\},$$

$$\sigma_s = 2\pi \int_0^R \left| 1 - \exp(-K + 2ik_1) S \right|^2 \rho d\rho \tag{8}$$

or

$$\frac{\sigma_s}{\pi R^2} = 1 + \frac{1}{2} x^{-2} \left\{1 - (1 + 2x) \exp(-2x)\right\}$$

$$- \left[\frac{1}{4} x^2 + y^2\right]^{-2} \left\{\left[\frac{1}{4} x^2 - y^2\right]\right.$$

$$+ \exp(-x) \left[2y\left(\frac{1}{4} x^2 + y^2\right) + xy\right] \sin 2y$$

$$\left. - \exp(-x) \left[\left(\frac{1}{4} x^2 - y^2\right) + x\left(\frac{1}{4} x^2 + y^2\right)\right] \cos 2y \right\},$$

where $x = KR$, $y = k_1 R$, $s^2 = R^2 - \rho^2$. The terms σ_s and σ_I from Eqs. (7) and (8) are given in Figs. 8 and 9 for various values of KR and $k_1 R$.

In addition to Eqs. (7) and (8) the optical model gives, for the scattering amplitude,

$$f(\theta) = k \int_0^R \left[1 - e^{(-K + 2 i k_1)S}\right] J_0(k \rho \sin \theta)\, \rho d\rho \,. \tag{9}$$

An approximate form for Eq. (9) is

$$f(\theta) = \frac{i}{2k} \sum_{\ell = 0}^{\ell m + 1/2 \leq kR} (2\ell + 1)(1 - e^{(-k + 2ik_1) S_\ell}) P_\ell(\cos \theta), \tag{10}$$

where

$$S_\ell = \left[k^2 R^2 - (\ell + 1/2)^2\right] / k.$$

This expression is also obtained by treating the complex square well in W.K.B. approximation.

Using the results of the optical model, we now write

$$a_i = \frac{\int_{\theta_i}^{\pi} \left[d\sigma(\theta)/d\omega\right] \sin \theta d\theta}{\int_0^{\pi} \left[d\sigma(\theta)/d\omega\right] \sin \theta d\theta} \tag{11}$$

and

$$\Delta a = \frac{\int_{\theta_1}^{\theta_2} \left[d\sigma(\theta)/d\omega\right] \sin \theta d\theta}{\int_0^{\pi} \left[d\sigma(\theta)/d\omega\right] \sin \theta d\theta} \tag{12}$$

where $d\sigma(\theta)/d\omega$ is the differential scattering cross section. Using $d\sigma(\theta)/d\omega = |f(\theta)|^2$, we find that a_i and Δa are nearly independent

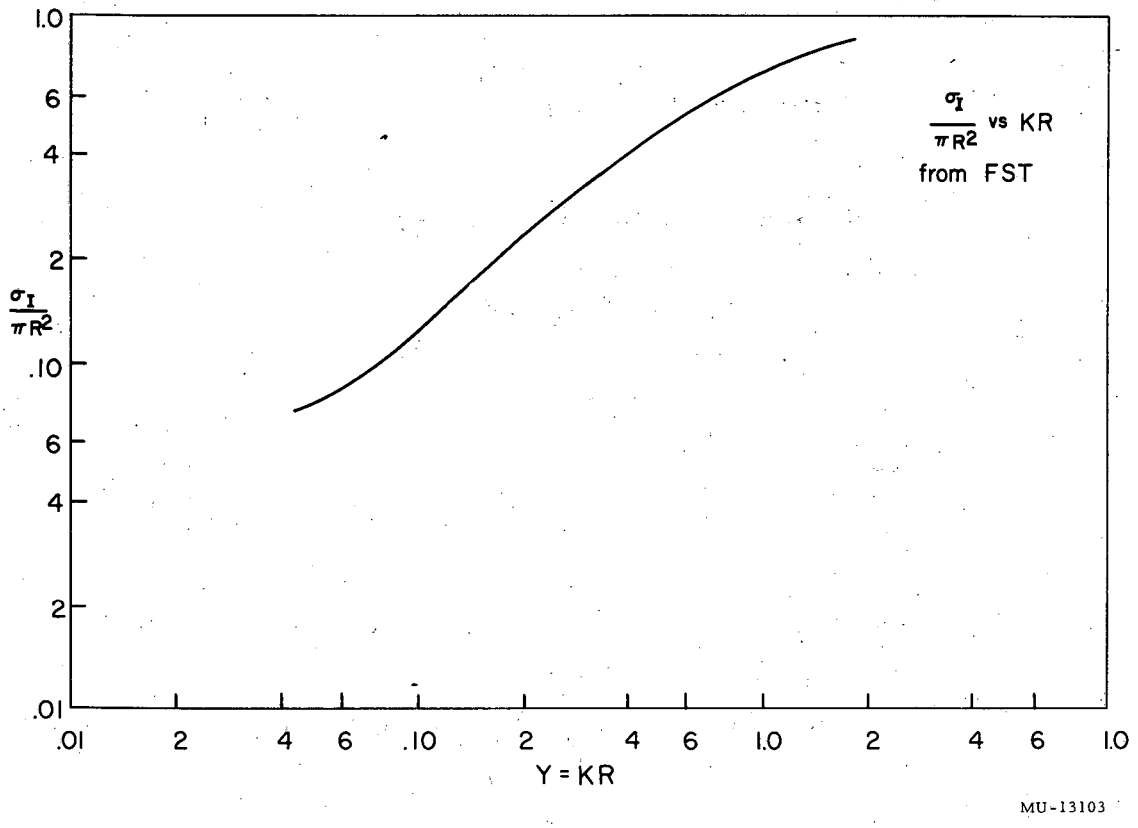

Fig. 8. Total interaction cross section as given by the optical model.

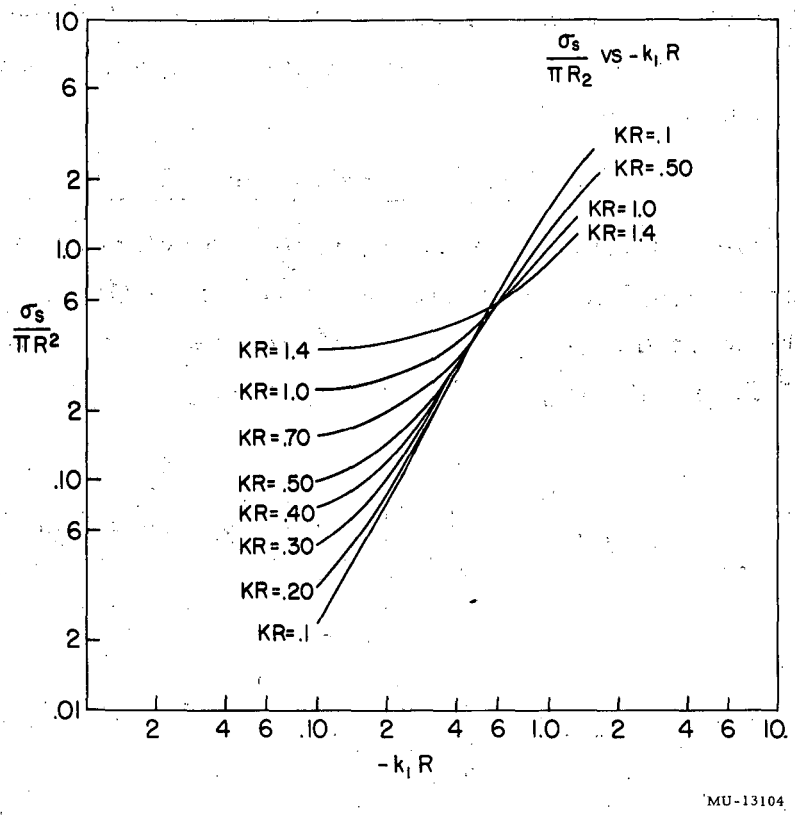

Fig. 9. Total scattering cross section as given by the optical model.

of KR and k_1R and are only a function of kR. It has been pointed out that such a conclusion is reasonable, since we expect the shape of $f(\theta)$ to depend most strongly on the number of partial waves included in the scattering.[11] In the first Born approximation, we find that the shape of $f(\theta)$ is absolutely independent of k_1 and K.

After final values for k_1 and K had been obtained, new a's and Δa's were calculated, and were found to differ from the previous values by less than 1% (see Section IV-E).

The above analysis is in the framework of Schroedinger wave mechanics, therefore not relativistically correct; however, relativistic kinematics were used.

C. Effect of the Coulomb Potential

In the analysis thus far, the Coulomb potential has been neglected. The potential of Eq. (4) should include the real Coulomb potential that exists between the two particles. If the first Born approximation is used,[13] the scattering amplitude is given by

$$f_c(\theta) = \frac{1}{K} \int_0^\infty r' \sin Kr' \, U(r') \, dr', \qquad (13)$$

where

$$U(r') = \frac{2E}{\hbar^2 C^2} V(r),$$

$$K = 2k \sin \theta/2.$$

As before, this treatment is nonrelativistic; however, relativistic kinematics were used. Now if $U(r')$ can be written as an integral taken over a density function $\rho(r)$ Eq. (13) becomes

$$f_c(\theta) = f_{0_c}(\theta) \, F(\theta), \qquad (14)$$

where $f_{0_c}(\theta)$ is the scattering amplitude derived from a point scatter

and $F(\theta)$ is the nuclear form factor. For Coulomb scattering, $f_{0_c}(\theta)$ and $F(\theta)$ are given [16] by

$$f_{0_c}(\theta) = \frac{-2 Z_e{}^2 E}{(\hbar c)^2 K^2} , \tag{15}$$

$$F(\theta) = \frac{4\pi}{K} \int_0^\infty \rho(r) \sin Kr \; r dr . \tag{16}$$

For a uniform charge distribution of radius R, Eq. (16) becomes

$$F(\theta) = 4\pi R^3 \left[\sin KR - KR \cos KR/(KR)^3 \right]. \tag{17}$$

Equations (15) and (17) give the scattering amplitude as calculated in the Born approximation. It is well known that the magnitude of $f(\theta)$ derived from the Born approximation is nearly exact; however, the phase is not correct. To estimate the maximum effect, the phase of $f_c(\theta)$ was arbitrarily taken to be the same as the phase of $f(\theta)$ given by Eq. (10) for the square well. For all values of K and k_1 that are of interest in the current problem, the Coulomb effect was found to be negligible.

D. Inelastic Scattering Correction

A K meson that inelastically scatters may still have sufficient energy to reach the S and A counters, or may give a star prong of sufficient range to count. The fraction of K particle giving rise to such events is the $1-\beta$ of Eq. (3). The β's calculated from nuclear emulsion data [16] were

$$\beta_1 = 0.91, \qquad \beta_2 = 0.81, \qquad \Delta\beta = 0.10. \tag{18}$$

The statistical accuracy of these numbers is about 5% for β_1 and β_2 and about 30% for $\Delta\beta$.

Justification for the use of results from nuclear emulsion for the lighter elements is dubious since β might well depend on the size of the nucleons. The effect of a variation in β on the determination of K and k_1 is discussed in Section IV-E.

E. Complex Square-Well Parameters

From Eqs.(3), (7), and (8), and the values of α and β, one can determine K and k_1 pairs that fit each measured cross section. Thus, for each target, three curves are constructed that give the values of K and k_1 appropriate to each of the measured cross sections. Figure 10 gives such curves for aluminum, and these are quite typical of the other targets. The dotted lines indicate the uncertainty in the various curves due to the statistical errors on the measured cross sections. As is expected, σ_1 and σ_2 are nearly independent of k_1, whereas $\Delta\sigma$ depends on both K and k_1.

The values of K and k_1 for each target as determined from the curves are given in Table II.

Table II

k_1 and K derived from the measured cross section (in units of 10^{13} cm^{-1})

	C	Al	Cu	Ag	Pb
$-k_1$	0.078±0.062	0.191±0.029	0.240±0.050	0.146±0.030	0.185±0.046
K	0.087±0.003	0.077±0.012	0.077±0.009	0.060±0.008	0.058±0.009

The errors shown reflect only the statistical inaccuracy in the measured cross sections. The systematic errors of the analysis are somewhat larger.

The uncertainty of extending a β determined for nuclear emulsion to lower Z has practically no effect on K; however it certainly affects k_1. The values of k_1 in Table II should be reliable to about ±50%. The values of K must be taken in the spirit of the square-well approximation and considered as only a first approximation to the real physical potential.

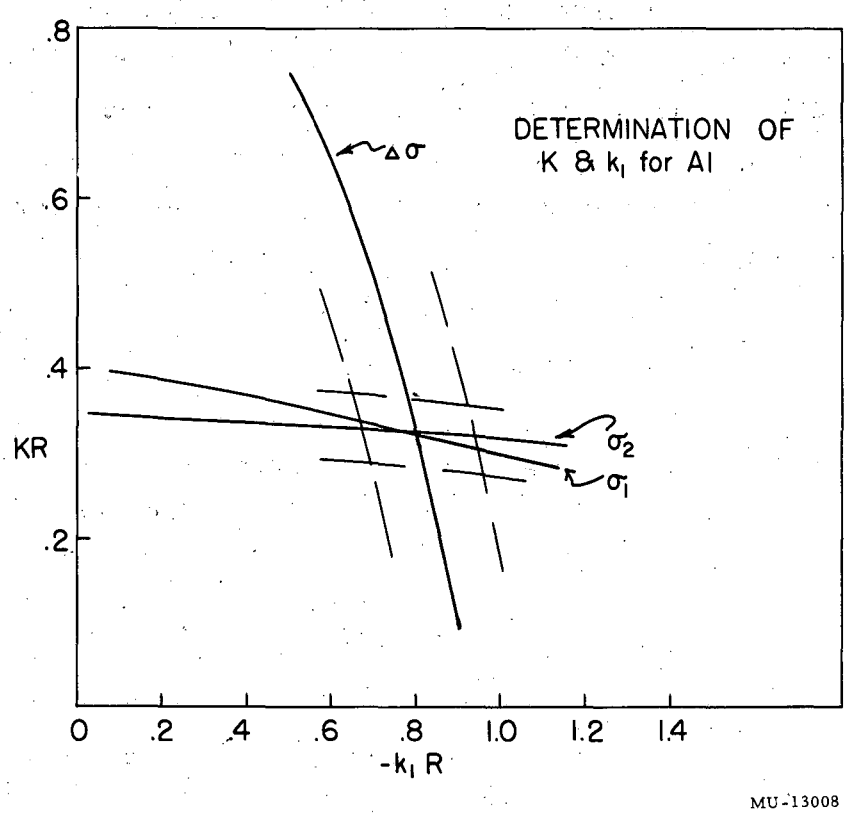

Fig. 10. Determination of K and k_1 for aluminum.

The values of the real potential derived from Eq. (6) by use of the values of k_1 given in Table II are shown in Fig. 11. The average potential is found to be 24.2 ± 2.3 Mev.

F. Mean Free Path for Interaction in Nuclear Matter

The problem of deriving the mean free path in nuclear matter from the individual K-nucleon interactions would still be a vastly difficult one, even if the basic interactions were understood. In the simplest picture, one assumes that each nucleon within the nucleus can interact with the K particle completely independently of the other nucleons. Thus, we may write the mean free path within the nucleus as

$$\lambda = K^{-1} = (\sigma_0 \rho)^{-1} , \tag{18}$$

where K is the absorption constant as defined in Section V-B, σ_0 the K-nucleon cross section, and ρ the nuclear density. For $R = r_0 A^{1/3}$, ρ is given by

$$\rho = \frac{3}{4} (\pi r_0^3)^{-1} . \tag{19}$$

The values of σ_0 that were obtained from Eqs. (18) and (19) by use of the values of K from Table II are shown in Fig. 12. Again the errors are purely statistical. The drop in the value of σ_0 for silver and lead, if significant, may indicate a failure of such a simple relation as Eq. (18).

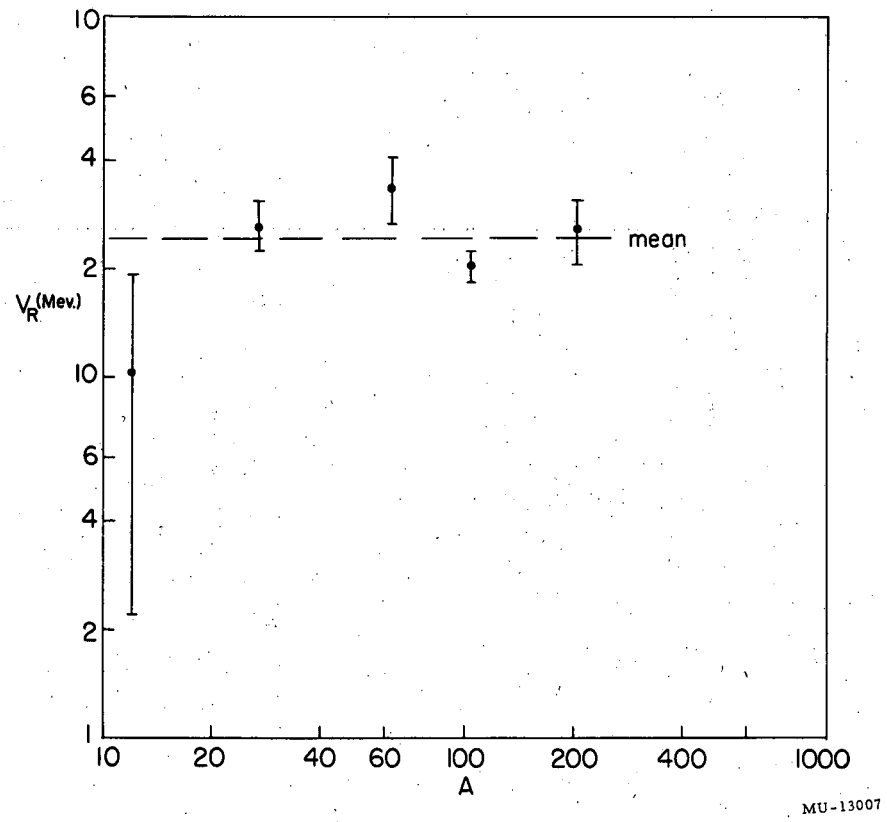

Fig. 11. Experimental values of V_1.

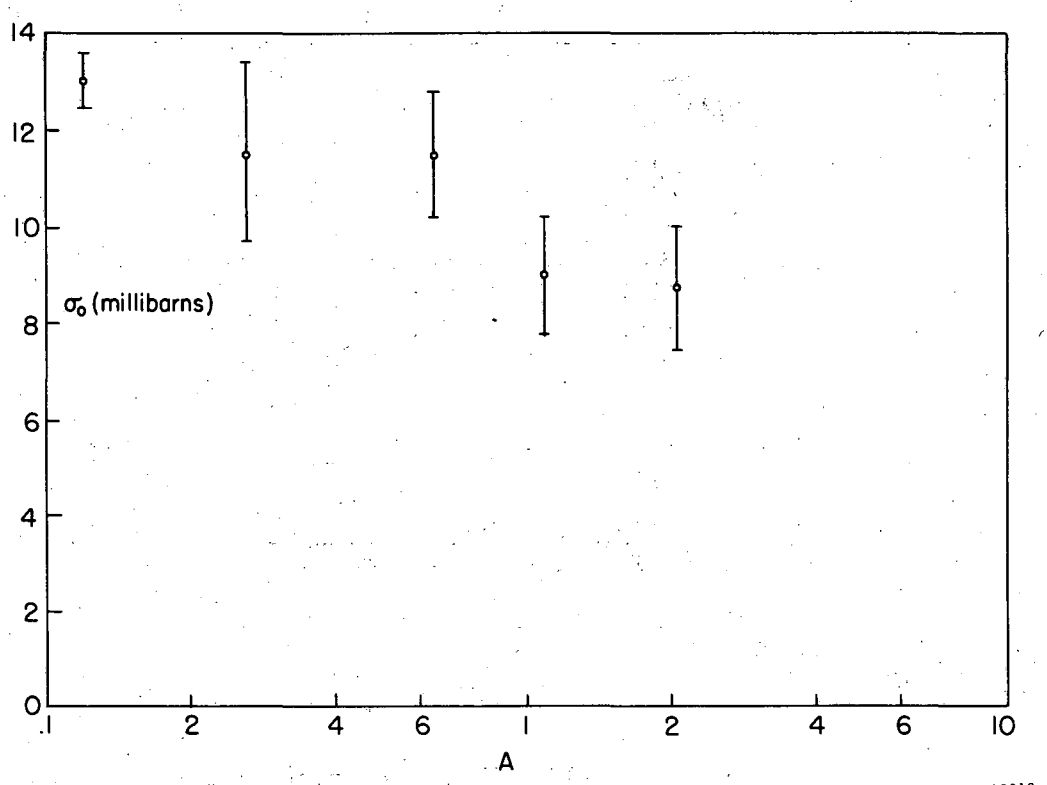

Fig. 12. Experimental results for σ_0.

V. DISCUSSION

A. Real Potential

The real potentials shown in Fig. 11 may be compared with results from experiments with nuclear emulsion[12, 17] for K mesons of lower energy. The values at low energy are about 10 to 15 Mev. Thus values here are significantly larger, indicating an increase of the real potential with increasing K energy. The results here are in reasonable agreement with preliminary nuclear emulsion results at similar energies.[18]

B. Absorption Constant

The value of σ_0 from Fig. 12 is lower than the K-proton cross section given by various nuclear emulsion groups. The apparent drop of σ_0 with increasing A, shown in Fig. 12, is not understood at present. Possible explanations follow in Sections 1 and 2 below.

1. Surface Effect

The interaction process of K particles in complex nuclei may actually be a surface effect. Similar assumptions have been necessary to explain low-energy neutron scattering.[19]

2. Effect of Magic Numbers

Since silver is nearly "magic" in proton number, and lead is doubly magic, one expects the lowest unoccupied level for a nucleon to be higher in silver and lead than in the lower-Z target. Thus, collisions with small energy transfer between the K and an internal nucleon might be more highly forbidden in silver and lead than in the other targets. This effect would be enhanced if the K-nucleon scattering were peaked forward.

3. Conclusion

Sections 1 and 2 above are mere conjectures. Any real belief in the dependence of the absorption constant on A should depend on further experiments.

ACKNOWLEDGMENTS

The assistance of Dr. Ludwig van Rossum and Mr. Thaddeus Kycia during all phases of the experiment--and at all hours of the day and night--is greatly appreciated. The experiment would have been impossible without the physical labor, freely contributed during the actual run, by Dr. Robert Birge, Dr. Marian Whitehead, Dr. Robert Lanou, Dr. Jack Sandweiss, Dr. Roy Haddock, Mr. Robert L. Fry, Jr., and Mr. Thomas T. Reynolds. The help of Mr. Robert Fry, Mr. Thomas Reynolds, Mrs. Marilynn Harbert, and Miss Betty Blaine in scanning the film is greatly appreciated. Dr. Donald Stork is thanked for valuable discussions during the initial stages of the experiment, and for the method of analysis taken from his doctoral dissertation. Dr. Jack sandweiss contributed many suggestions during the analysis.

The tolerance of my family--Ruth, Norman, Randall, and Christine--contributed immeasurably to the success of the experiment. Dr. Edward J. Lofgren and the operating crew of the Bevatron are to be thanked for efficient and effective operation of the machine. The IBM 650 computer is to be acknowledged for some several million arithmetical operations.

This work was done under the auspices of the U.S. Atomic Energy Commission.

APPENDIX

A. Statistical Standard Deviation of the Measured Cross Sections

Consider N_0 particles incident on the target. We ask what is the probability that N particles leave the target when the average number is $\bar{N}$. Now, the probability of having the first N particles penetrate the target and the next $(N_0 - N)$ particles not get through is given by

$$P_+^{\,N} (P_-)^{N_0 - N} ,$$

where P_+ is the probability that a particle gets through, or

$$P_+ = \frac{\bar{N}}{N_0} \quad \text{and} \quad P_- = (1 - P_+) .$$

Now the number of ways of arranging the N particles among the N_0 particles is just $N_0(N_0-1)\,(N_0-2)\ldots\ldots(N_0-N+1)$, and the number of ways of interchanging the N particles in $N!$. Thus, we have

$$P(N) = \frac{N_0!}{(N_0-N)!\;N!}\; P_+^{\,N} (1 - P_+)^{N_0 - N} ,$$

which is just the binomial distribution. For large N and N_0, $P(N)$ approaches a normal distribution of standard deviation:

$$\Delta = \sqrt{N_0 P_+ P_-} .$$

Now, by Eq. (1) we have

$$\sigma_i = \frac{1}{\eta} \left(\ln \frac{N_0}{N_i} - \ln \frac{N_0'}{N_i'} \right) ;$$

thus

$$\Delta_\sigma = \sqrt{\frac{1}{N_0} - \frac{1}{N_i} + \frac{1}{N_0'} - \frac{1}{N_i'}} .$$

B. The Uncorrected Data

Uncorrected data from which the cross sections of Table I were calculated are as follows.

	Target thickness in g/cm^2	η $(\times 10^{23})$	$\Sigma_1 = \ln N_0/N_1$ $(\times 10^{-4})$	$\Sigma_2 = \ln N_0/N_2$ $(\times 10^{-4})$
C	10.39	5.19	90.6	57.1
Al	11.86	2.65	96.4	53.3
Cu	13.04	1.235	102.8	61.5
Ag	15.817	0.883	87.7	53.8
Pb	18.75	0.544	100.1	54.7
Background	0	0	40.5	14.0

REFERENCES

1. See for instance, Pisa Conference Report; Nuovo Cimento Suplemento, Vol. IV, No. 2 (1956).
2. Widgoff, Shapiro, Schluter, Ritson, Pevsner, and Henri, Phys. Rev. 104, 811 (1956).
3. Courant, Livingston, and Snyder, Phys. Rev. 88, 1190 (1952).
4. Kerth, Stork, Birge, Haddock and Whitehead, Bull. Am. Phys. Soc. 30, No.3,41(1955).
5. B. Youtz, Scattering of 90-Mev Neutrons by Deuterons (Thesis) UCRL-2307, Aug. 1953.
6. V. Fitch and R. Motley, Phys. Rev. 101, 496 (1956).
7. Radiation Laboratory Counting Handbook, UCRL-3307, Jan. 1956.
8. R.L. Garwin, Rev. Sci. Instr. 24, 618 (1953).
9. Alvarez, Crawford, Good and Stevenson, Proceedings of the Sixth Annual Rochester Conference on High-Energy Physics, Interscience, New York, (1956).
10. E. Fermi, Nuclear Physics, Revised Edition (University of Chicago Press, Chicago, 1950).
11. D.H. Stork, Phys. Rev. 93, 868 (1954).
12. D. Fournet Davis (to be published); J.E. Lannutti (private communication).
13. L.I. Schiff, Quantum Mechanics (McGraw-Hill, New York, 1949).
14. N.C. Francis and K.M. Watson, Am. J. Phys. 21, 659 (1953); Fernbach, Serber, and Taylor, Phys. Rev. 75, 1352 (1949).
15. Mac Born, Optik Springer, (Berlin, 1933).
16. L.T. Schiff, Phys. Rev. 92, 988 (1953); M.E. Rose, Phys. Rev. 73, 279 (1948).
17. D.H. Perkins (private communication).
18. J.E. Lannutti (private communication).
19. S. Fernbach (private communication).